Chapter 7

7. Estimation of Abutment Angle for Varying Geo-Mining Conditions

7.1 General

This chapter describes the results of three-dimensional numerical modelling to determine the abutment angle for different geo-mining conditions. The term 'abutment angle' in this study refers to the angle subtended by the caving line and the vertical plane at the edge of the longwall panel. The procedure of three-dimensional numerical modelling followed Behera (2022). The model can simulate the caving phenomenon of the roof strata with the progressive retreat of the longwall face and accurately model the major weighting cycles as verified against the field observations for typical longwall workings in Indian geo-mining conditions.

It is hypothesised that the modelling procedure, with the capabilities mentioned above, can be used for determining abutment angle as it correctly models the caving process and load on powered supports, which is fundamentally a manifestation of strata response in the caving zone. The modelling scheme and its formulation have been discussed in Section 3.13, Chapter 3. This study also considered the abutment angle as a physical reality in place of a mathematical entity to approximate the side abutment load, as considered in several previous studies (Mark, 1992; Colwell et al., 2003; Tulu and Heasley, 2012; Hill et al., 2015; Tuncay et al., 2021).

7.2 Mechanism of Abutment Angle Formation

Before the occurrence of any caving, the immediate roof strata behave like a fixed-ended beam for a specific span of face advance, depending upon the geology and physico-mechanical properties of the rock beds. With an increase in the span, the curvilinear cracks cut through the

beds and transform the fixed-ended beam into the simply supported beam (Das 2000). The beam remains unsupported as the face retreats further and is broken into rock fragments of various sizes as it falls (Figure 7.1). The cantilever formed in the process is shortened in length as shear cracks cut through it. The cantilever either overhang or cut just at the chain pillar edge, depending upon the presence of geological disturbances and properties of the overlying beds. A similar process is sequentially repeated for all the rock beds. The length of the cantilever of the upper strata is either the same or greater than the cantilever of the lower strata, depending on their bending behaviour. In this process, an abutment is formed about the chain pillars. This abutment leads to increased loading and confinement to the pillar (Chokhani, 2012). Hence, the stability of the pillar is significantly influenced by the abutment angle.

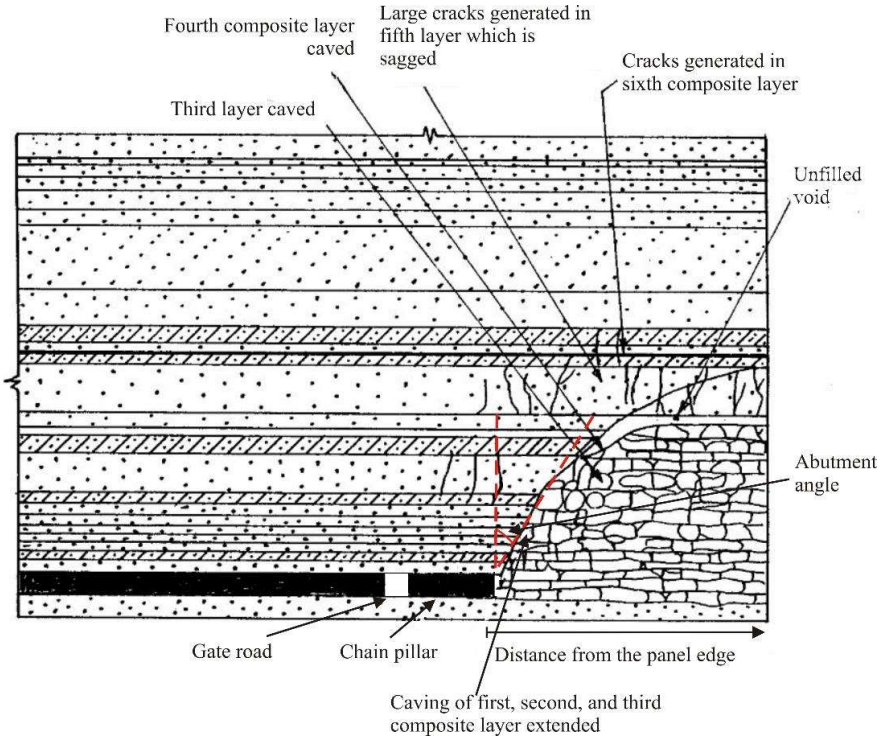

Figure 7.1 Formation of abutment along the panel edge in a typical longwall working

7.3 Identification of Parameters affecting Abutment Angle

In past studies, the abutment angle has been used to determine the load on the chain pillars using the simplified two-dimensional subsidence model (Wilson, 1972b; King and Whittaker, 1971; Choi and McCain, 1980). These studies suggested an abutment angle of 17 - 31° for different geo-mining conditions. Mark (1990) opined that although the abutment angle varied from 10.7 to 25.2°, the average abutment angle of 21° provided a conservative estimate of side abutment load in US coalfields. The face length in these workings varied from 143 to 305 m, while the depth of cover ranged between 139 to 232 m.

The study of side abutment loading in Australian conditions (Colwell 1998) showed that the measured abutment load and its extent could deviate significantly from the estimates of the empirical formula in ALPS (Mark 1990) that uses a constant abutment angle of 21°. Several studies (Lawson et al. 2017, Reed et al. 2017, Singh and Singh 2009) have highlighted that the load transfer and the stress concentration are greatly influenced by the presence of strong and stiff rock units, their thickness and location within the active caving zone of strata. The massive and stiff strata can transfer loads to greater distances and reduce the stress recovery in the goaf by resisting caving. Singh and Singh (2009) and Obert and Duvall (1967) noted that the effective unit weight and equivalent tensile strength of the rock layers within the caving zone significantly influence the caving process and, therefore, the spans of major roof caving.

Based on a recent study at 12 mines in Australian and the US conditions, Tuncay et al. (2021) reported that the abutment angle significantly depends on the panel depth to width ratio. The abutment angle varied from 6.33 to 23.39° for cover depth and panel width range of 125 – 625 m and 130 – 275 m, respectively. In another study at 30 US and Australian coal mines, Tulu and Heasley (2012) observed that the abutment angle decreases with increasing cover depth. It ranged from 6 to 18° for a cover depth of 274 – 625 m.

Based on the field observation in the Indian geo-mining conditions, Das (2000) noted that the caving angle (complimentary angle of the abutment angle) depends on the strata formation and strength. He opined that the caving angle could be less than 30° for very thick, strong, and massive sandstone strata and can go up to 90° for extremely weak strata formation.

The findings of these studies show that the abutment angle is not a constant entity. It varies with the nature of strata formation, cover depth, panel width, thickness and sequence of rock units within the active caving zone and the stiffness of the overburden strata.

7.4 Numerical Modelling Study

A parametric study was designed based on three-dimensional numerical modelling to assess the influence of several geo-mechanical and mining parameters on the abutment angle. The range of the parameters was derived based on the properties of the coal and the coal measure rocks in 27 longwall workings in different coalfields in India. The collated database of these longwall panels is described in Table 8.1, Chapter 8. The parameters considered in this study included cover depth, face length, strength and deformation modulus of the strata, and the thickness of the immediate and the main roof layers. It aimed to assess the variation in abutment angle with the change in these parameters.

The parametric study was designed keeping in mind the prevailing and the anticipated future scenario of longwall workings in the Indian condition. Figure 7.2 illustrates the range of cover depth and thickness ratio parameters considered in this study. The study was conducted for three cover depths: 350, 600, and 900 m, while the thickness ratio (ratio of the thickness of the main roof to the immediate roof) varied from 0.5 to 2.0, maintaining the total caving height of 15 times the extraction height. The range of the remaining parameters is shown in Figure 8.1, as they are common for both studies.

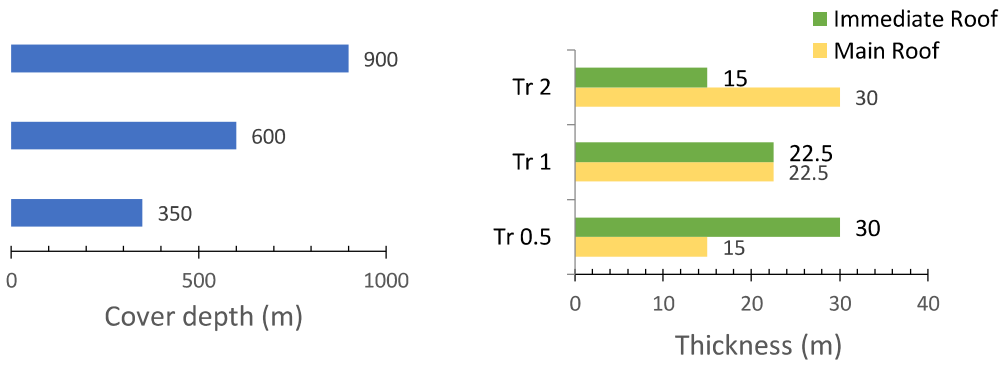

(a) (b)

Figure 7.2 Variation of (a) cover depth and (b) thickness ratio for estimation of the abutment angle

The face length varied from 150 - 250 m. Based on the range of compressive and tensile strengths of the strata and the coal seam, the strata and the seam were categorised into soft, moderate and hard. The compressive strength of the immediate roof ranged from 4.01 to 20.92 MPa, while for the main roof, it varied from 4.11 to 17.58 MPa. The immediate roof tensile strength varied from 0.39 to 2.39 MPa, while the main roof tensile strength varied between 0.35 - 2.12 MPa. Similarly, the elastic modulus of the immediate roof and the main roof ranged from 3.01-13.37 MPa and 3.86-13 MPa, respectively.

The base model considered extraction of a 3m thick coal seam under a 15 m thick immediate roof and 30m thick main roof. The thickness of the overburden strata was 150 m. The vertical stress equivalent to the load of the remaining overburden was initialised at the top of the model. The thickness of the floor was taken as 100 m in the model. The rock mass properties were estimated using the approach suggested by Singh and Singh (2009), while the in-situ stress estimates obtained by Equations 3.24 and 3.25 was initialised in the model. The coal seam was progressively mined till the completion of the mail fall in the goaf. The abutment angle was measured at the panel edge by considering a vertical section normal to the face length passing

through the middle of the face. A total of 81 three-dimensional experimental models were studied.

7.5 Model Observations

The abutment angle was measured at the edge of the barrier pillar beside the set up/installation chamber of the panel, assuming that the angle so measured would be similar to the angle measured at the edge of the chain pillar away from the influence of face. A vertical section was defined at the middle of the face length for the measurement of the abutment angle. Figure 7.3 illustrates the measured abutment angle in two experimental workings with soft and hard strata conditions with a face length of 200 m, cover depth of 600 m, and thickness ratio of 2. The abutment angle was measured when the main roof had wholly caved in the goaf upon completion of the main fall. At this point, the pile of the caved goaf is considered to establish contact with the overburden strata and receive compaction with the subsequent face retreat. The abutment angle measured at the starting line of the panel was assumed to remain independent of the main fall or periodic caving and the cumulative face advance. Table AIV.1 (Annexure-IV) shows the measured abutment angle for the experimental conditions.

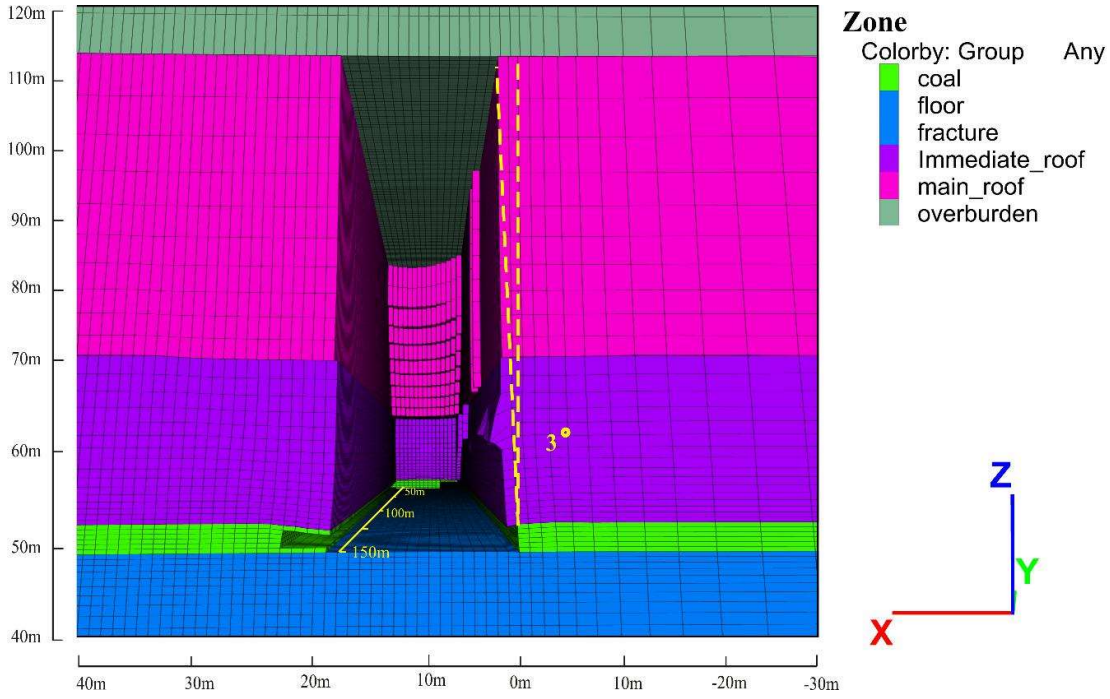

(a)

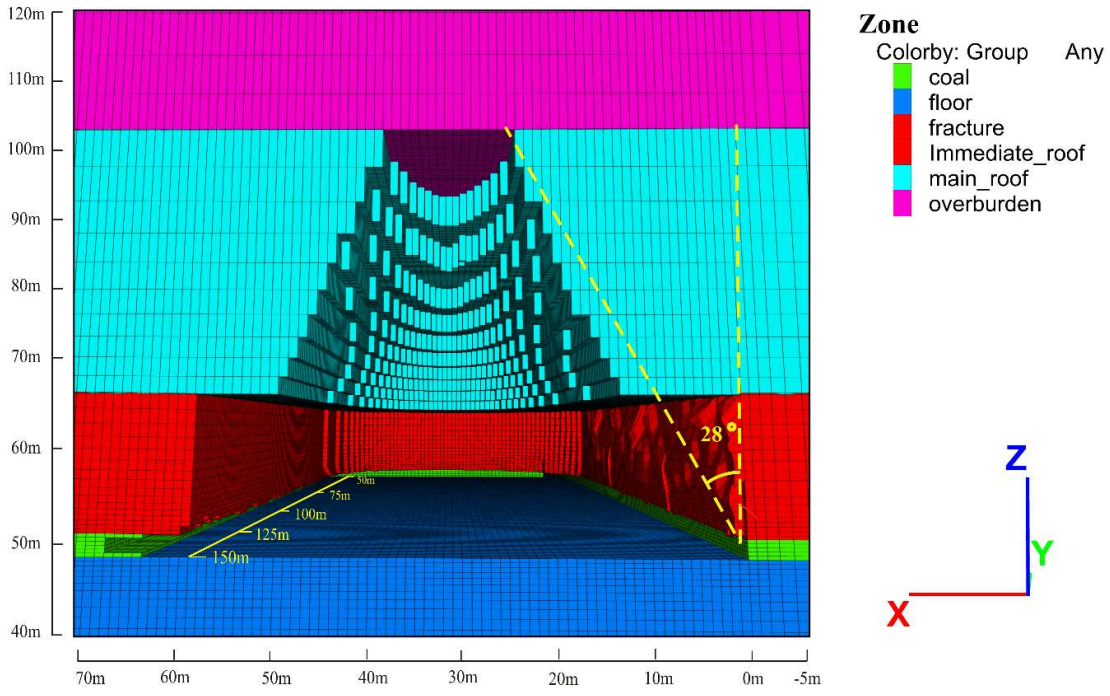

(b)

Figure 7.3 Three-dimensional view of the measured abutment angle in case of experimental models with (a) soft strata and (b) hard strata conditions at the cover depth of 600 m with face length of 200 m and thickness ratio of 2

The abutment angle varied from 10 to 25° for the decrease in the face length from 250 m to 150 m at the cover depth of 600 m in the moderate strength condition of the strata with the thickness ratio of 1.0. With a change in the cover depth from 350 m to 900 m, the abutment angle decreased from 38° to 5° for the moderate strength condition, face length of 200 m, and thickness ratio of 1.0. However, the abutment angle increased from 8 to 32° for the strength changing from soft to hard at the cover depth of 600 m, face length of 200 m, and the thickness ratio of 1.0. At the cover depth of 600 m, face length of 200 m, and moderately strong strata condition, the maximum and the minimum abutment angle of 18° and 3° were observed for thickness ratios of 1.0 and 0.5, while the abutment angle was 7° for the thickness ratio of 2.0.

The analysis of the model results showed that the abutment angle is significantly influenced by the cover depth, strata condition, face length, and thickness ratio. A consistently decreasing trend in the abutment angle can be observed with an increase in the cover depth across the strata condition, face length, and thickness ratio (Figure 7.4).

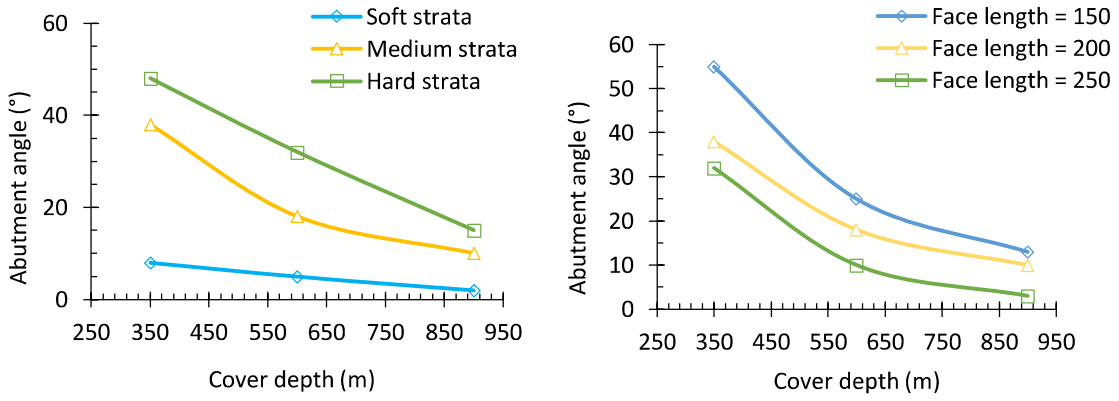

(a) (b)

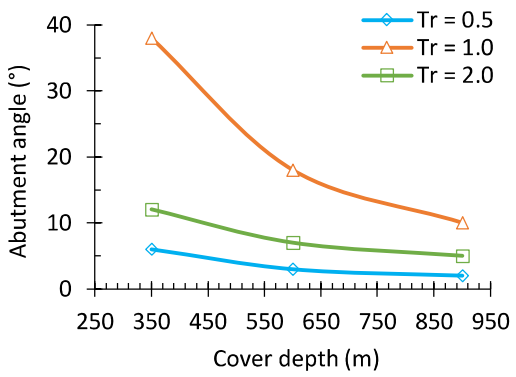

(c)

Figure 7.4. Variation of the model observed abutment angle with (a) the cover depth and strata condition, (b) the cover depth and face length, and (c) the cover depth and thickness ratio.

Figure 7.4 (a) shows the variation of the abutment angle with the strata condition and cover depth for the face length of 200 m and thickness ratio of 1. It can be seen that the abutment angle varied from 8° for soft strata to 48° for hard strata condition at the cover depth of 350 m, whereas it ranged from 2° for soft strata to 15° for hard strata condition at 900 m depth. A wide variation in the abutment angle from 48° at 350 m to 15° at 900 m depth was noted for the hard strata condition. The variation was relatively narrow, from 8° at 350 m to 2° at 900 m depth for the soft strata condition. The abutment angle showed very high sensitivity to the geo-mechanical properties of the strata.

Figure 7.4 (b) depicts the variation of the abutment angle with the face length and cover depth for the thickness ratio of 1 and moderate strength strata. It can be seen that the abutment angle reduced from 39 to 20° as the face length was increased from 150 m to 250 m at the cover depth of 350 m. The angle reduced from 7° to 4° with the increase in face length from 150 m to 250 m at 900 m depth. Hence, at a relatively smaller depth of 350 m, the abutment angle is

more sensitive to the change in face length than the high cover depth of 900 m, where the abutment angle was only marginally affected by an increase in the face length.

Figure 7.4 (c) shows the variation of the abutment angle with the thickness ratio (Tr) and cover depth for the face length of 200 m and moderate strata condition. It can be seen that the abutment angle reduced from 16° to 4° with the increase in cover depth from 350 m to 900 m for Tr=0.5. The abutment angle reduced from 42° to 10° as the cover depth increased from 350 m to 900 m for Tr = 1.0. Similarly, the abutment angle reduced from 28° to 4° with the increase in the cover depth from 350 m to 900 m for Tr=2.0. At a given depth of cover, the abutment angle was maximum for Tr = 1.0, where the thickness of the immediate and the main roofs was the same. The abutment angle was minimum for Tr = 0.5, when the thickness of immediate roof was 30 m and the main roof was 15 m. Hence, the thickness of the immediate and the main roofs significantly affected the abutment angle. The abutment angle was maximum at a given depth when the immediate and the main roof were equally thick.

7.6 Statistical Model for Estimation of the Abutment angle

The findings of the parametric study suggested that the cover depth, thickness and geo-mechanical properties of the immediate and main roof layers substantially influence the abutment angle. Earlier, the literature review confirmed a significant effect of the unit weight and the tensile strength of the immediate and main roof layers on the abutment angle (Section 7.3). Hence, a statistical model (Equation 7.3) was developed considering the cover depth and face length in addition to the thickness, the equivalent tensile strength and the effective unit weight of the immediate and main roof layers. The effective unit weight of a rock layer can be determined using Equation 7.1.

$$\gamma = \frac{E_1 t_1^2 (\gamma_1 t_1 + \gamma_2 t_2 + \ldots)}{(E_1 t_1^3 + E_2 t_2^3 + \ldots)} \quad (7.1)$$

where, γ is the effective unit weight in MPa/m, γ_1, γ_1, … are the unit weight of rock layers, E_1, E_2, are Young's modulus of rock layers, and t_1, t_2 ... are the rock layers thickness.

The equivalent tensile strength of the roof layers for the main fall was estimated by Equation 7.2, which considered the intact rock tensile strength (σ_t), the mean in-situ horizontal stress ($\boldsymbol{\sigma_h}$) and the RQD of the roof layers. The RQD value of the layer accounted for the strength degradation due to the presence of geological discontinuities, such as joints and bedding planes. The horizontal stress and tensile strength resist the bending and failure of the layers. Equation 7.2 combined the effect of these parameters. In the absence of the field measured values, the average in-situ horizontal stress was estimated using Equation 3.24.

$$\boldsymbol{\sigma_m} = \frac{(\boldsymbol{\sigma_t} + \boldsymbol{\sigma_h})\mathbf{RQD}}{\mathbf{100}} \quad (7.2)$$

where, RQD is the Rock Quality Designation, %.

The minimum, maximum, mean, and standard deviation of the values of the parameters for all the 81 data sets of the parametric models and the abutment angle are summarised in Table 7.1.

Table 7.1 Statistical summary of the considered parameters in the model

Variable	Minimum	Maximum	Mean	Std. deviation
Abutment angle (°)	1	85	19.049	17.521
Face length (m)	150	250	200	41.079
Depth (m)	350	900	616.667	226.247
σm (Main roof)	1.915	14.279	8.284	5.086
σm (Immediate roof)	1.476	14.026	7.817	5.156
Tmr (m)	15	30	22.5	6.162
Tir (m)	15	30	22.5	6.162
Unit weigth (Main roof), MPa/m	0.019	0.023	0.021	0.002
Unit weigth (Immediate roof), MPa/m	0.018	0.031	0.023	0.004

The above parameters were transformed into the logarithmic scale to conduct the multiple linear regression (MLR). The coefficient and intercept values of the regression study were then utilised to develop Equation 7.3.

$$\boldsymbol{\beta = 108.57 F_L^{-0.5} H^{-1.57} \left(\frac{\sigma_{mIR} T_{IR}}{\gamma_{IR}} \times \frac{\sigma_{mMR} T_{MR}}{\gamma_{MR}} \right)^{0.58}} \quad \boldsymbol{, R^2 = 0.7918} \qquad (7.3)$$

where, β is the abutment angle (°), F_L is the face length (m), H is the cover depth (m), σ_{mIR}, σ_{mMR} are the equivalent tensile strength of the immediate roof and main roof (MPa), respectively, T_{IR}, T_{MR} are the thickness and γ_{IR}, γ_{MR} are the effective unit weight of the immediate roof and the main roof, respectively.

The proposed relation shows that the abutment angle is positively correlated with the thickness and the equivalent tensile strength of the roof layers, whereas it is negatively correlated with the cover depth, face length, and the unit weight of the roof layers. Further, 79.18% of the variability in the dependent variable is explained by the independent variables considered in the study.

7.7 Model Verification

Table 7.2 summarises the comparison of the model observed abutment angle with the data reported by Das (2000) in Indian longwall workings. The range of the model observed abutment angle is in close agreement with Das (2000). Further, the model estimated abutment angle decreased with the increase in cover depth following a power law, which agreed well with the previous studies (Tulu and Heasley 2012, Hill et al. 2015, Tuncay et al. 2021). The broader findings explaining the influence of the face length and the thickness ratio on the caving behaviour of the strata are also in line with the results of Singh and Singh (2009).

Table 7.2 Comparison of the model estimated abutment angle with the findings of Das (2000) in Indian longwall workings

Strata conditions	Depth (m)	Model observed abutment angle (°)	Field observations
Soft (RQD_{IR} = 47, RQD_{MR} =57 σ_{IR} = 20.55 MPa, σ_{MR} = 20.05MPa)	350	1-18	< 5-15°, for extremely cavable strata involving extremely weak strata including very weak composite and sandstone layers and for highly cavable strata involving very weak sandstone, soft and weak carbonaceous shale, very soft and fractured intercalation
	600	1-8	
	900	1-3	
Medium (RQD_{IR} = 76, RQD_{MR} =81 σ_{IR} = 58.4 MPa, σ_{MR} = 62.25 MPa)	350	6-55	< 15-55°, for moderately stronger very good cavable strata, good cavable strata, and poorly cavable strata involving shale sandstone, weak sandstone, intercalated shale and sandstone, hard, grey shale, medium-strength sandstone, quite strong sandstone, and medium strength massive sandstone
	600	2-25	
	900	2-13	
Hard (RQD_{IR} = 97, RQD_{MR} =98 σ_{IR} = 104.6 MPa, σ_{MR} = 87.9 MPa)	350	27-75	>40-60°, for poorly uncavable, highly uncavable and extremely uncavale strata involving quite strong sandstone, medium-strength massive sandstone, very thick massive sandstone, very strong sandy shale, competent and fine-grained sandstone with shale lamination, and very thick strong massive sandstone.
	600	6-38	
	900	2-27	

7.8 Summary

In this chapter, three-dimensional modelling-based parametric study was carried out to evaluate the effect of various geo-mechanical and mining parameters on the abutment angle. A well-validated three-dimensional numerical modelling procedure was adopted to simulate

progressive caving of the roof rocks, as detailed in Behera (2022) and evaluate the effect of cover depth, face length, strength of the roof layers, and thickness of the immediate and the main roof layers. The variation in these parameters was made considering the prevailing strata conditions in the Indian geo-mining conditions. A total of 81 three-dimensional models were studied, considering the range of variation in these parameters.

The results showed that the abutment angle was significantly dependent on the strata condition, cover depth, face length and thickness ratio of the roof layers. The abutment angle decreased with the increase in the cover depth, but increased with the increase in the strength of the roof layers. Its value decreased with the increase in the face length. The abutment angle was maximum for the thickness ratio of 1, whereas it was minimum for the thickness ratio of 0.5. The abutment angle varied from 1-75° depending upon the strata condition, cover depth, face length, and thickness ratio.

A statistical model was developed to predict the abutment angle in a given geo-mining condition. The model estimates were verified against the field observations in Indian conditions and the findings of the previous studies. The results corroborated well with the earlier findings.